[CANCER RESEARCH 63, 5428–5437, September 1, 2003]

A Molecular Fingerprint for Medulloblastoma[1]

Youngsoo Lee, Heather L. Miller, Patricia Jensen, Roberto Hernan, Michele Connelly, Cynthia Wetmore, Frederique Zindy, Martine F. Roussel, Tom Curran, Richard J. Gilbertson, and Peter J. McKinnon[2]

Departments of Genetics and Tumor Cell Biology [Y. L., H. L. M., F. Z., M. R., P. J. M.] and Developmental Neurobiology [P. J., R. H., M. C., T. C., R. G.], Saint Jude Children's Research Hospital, Memphis, Tennessee 38105, and Division of Pediatric Hematology/Oncology, Mayo Clinic, Rochester, Minnesota 55905 [C. W.]

ABSTRACT

Medulloblastoma is the most common malignant pediatric brain tumor. In mice, *Ptc1* haploinsufficiency and disruption of DNA repair (DNA ligase IV inactivation) or cell cycle regulation (Kip1, Ink4d, or Ink4c inactivation), in conjunction with p53 dysfunction, predispose to medulloblastoma. To identify genes important for this tumor, we evaluated gene expression profiles in medulloblastomas from these mice. Unexpectedly, medulloblastoma expression profiles were very similar among tumors and also to those of developing cerebellum. However, 21 genes were specifically up-regulated in medulloblastoma, including *sFrp1*, *Ptc2*, and *Math1*, members of signaling pathways that regulate cerebellar development. Coordinated deregulation of these same genes also occurred in a large subset of human medulloblastomas. These data identify a group of genes that is central to medulloblastoma tumorigenesis.

INTRODUCTION

Medulloblastoma, a highly invasive brain tumor that arises in the cerebellum, is the most common malignant pediatric brain tumor. Histopathologically, this disease is characterized by sheets of small round blue cells that are punctuated by frequent mitoses, apoptosis, and regions of divergent differentiation (1). Although the cell of origin for medulloblastoma is unknown, granule cell-precursor cells in the external germinal layer of the developing cerebellum are likely candidates (2). The treatment of medulloblastoma includes surgery, neuraxis radiation, and systemic chemotherapy that together cure only 60% of patients. Attempts to further reduce the morbidity and mortality associated with medulloblastoma have been restricted by the toxicity of conventional treatments and the infiltrative nature of the disease. Therefore, the availability of medulloblastoma model systems that can provide greater understanding of the molecular abnormalities that cause this tumor will be important for developing new strategies and approaches to treatment.

Signaling pathways that regulate normal cerebellar development such as the SHH[3] and WNT pathways have been linked to medulloblastoma tumorigenesis (2, 3). SHH and WNT proteins compose two families of secreted molecules that are required for cell growth and fate determination in many tissues including the nervous system (4–7). Germ-line mutation of *PTC1*, the receptor for SHH, is responsible for Gorlin syndrome, a familial cancer predisposition syndrome with a high incidence of medulloblastoma (8). Mutation of *PTC1* also occurs in sporadic medulloblastoma, and germ-line and somatic mutations of Suppressor of Fused, a downstream negative regulator of the SHH pathway, were reported recently in children with medulloblastoma (9). Up-regulation of SHH target genes, such as the transcription factor *GLI1*, also occur in medulloblastoma (2, 10). Similar to Gorlin syndrome, *Ptc1* haploinsufficiency in the mouse can lead to medulloblastoma, underscoring the direct relationship between SHH/PTC1 signaling and medulloblastoma (11–13).

The WNT pathway regulates β-catenin, a key transcriptional activator, via a multimeric protein complex that includes the APC tumor suppressor protein, GSK-3β (a serine-threonine kinase), and Axin (5, 14, 15). WNTs bind to the Frizzled family of receptors and inhibit GSK-3β-mediated phosphorylation and degradation of β-catenin. This enables translocation of β-catenin to the nucleus, where it activates the T-cell factor/lymphoid enhancer factor transcriptional complex, thereby up-regulating target genes that include *cyclin D1* and c-*MYC* (16). Deletion and/or mutations in *APC*, *AXIN1*, or *β-catenin* have been reported in sporadic medulloblastoma, and germ-line mutation of *APC* predisposes to medulloblastoma in Turcot's syndrome (17–21). Recent studies suggest a strong interrelationship between SHH and WNT signaling, with the phosphorylation status of GSK-3β acting as a signaling nexus between the two pathways (7, 22). Thus, during development the SHH and WNT pathways act as important tumor suppressor pathways in the cerebellum.

Defects in DNA repair, or defective responses to DNA damage, predispose to cancer (23). For example, mismatch repair defects are associated with colorectal cancer (24), whereas leukemia or lymphoma occurs in human syndromes associated with deficiencies in the response to DNA double-strand breaks, such as ataxia-telangiectasia and Nijmegen breakage syndrome (23). Recent evidence indicates that brain tumors may also arise in association with defects in the DNA damage response. In this regard, mice with DNA ligase IV or Parp1 deficiency have a high incidence of medulloblastoma (25, 26). DNA damage responses are also important in other pathways linked to medulloblastoma; $Ptc1^{+/-}$ mice are hypersensitive to ionizing radiation, and the incidence of medulloblastoma in these mice is dramatically increased after ionizing radiation (27–29). Thus, genotoxic stress may feature in the etiology of medulloblastoma.

Mouse models that recapitulate human disease have provided an enormous benefit toward molecular understanding of tumor biology. However, only recently have a number of mouse models of medulloblastoma become available (13, 25, 26, 30, 31). The defined genetics coupled with the ready accessibility of tissues, even at early developmental stages, are major advantages of mouse models. In this study, we have used a number of different mouse models for medulloblastoma to identify genes that may be important for the genesis of medulloblastoma. We identified a cohort of genes selectively up-regulated in all of the mouse medulloblastomas examined, as well as in a large subset of human medulloblastomas, thus providing new molecular insights into this tumor.

MATERIALS AND METHODS

Animal Tissue. $Lig4^{-/-}p53^{-/-}$, $Ptc1^{+/-}$, and $Ptc1^{+/-}p53^{-/-}$ mice have been described previously (13, 25, 30). $Ink4d^{-/-}Kip1^{+/-}p53^{-/-}$ and $Ink4d^{+/+}Kip1^{-/-}p53^{-/-}$ animals were obtained by intercrossing of $Ink4d^{+/-}Kip1^{+/-}p53^{-/-}$ animals, and $Ink4c^{-/-}p53^{-/-}$ and $Ink4d^{+/-}Ink4c^{-/-}p53^{-/-}$ animals were from intercrossing of $Ink4d^{+/-}Ink4c^{+/-}p53^{-/-}$ animals (32–34). All

Received 5/2/03; revised 6/12/03; accepted 6/17/03.

The costs of publication of this article were defrayed in part by the payment of page charges. This article must therefore be hereby marked *advertisement* in accordance with 18 U.S.C. Section 1734 solely to indicate this fact.

[1] Supported by NIH Grants CA-096832, NS-37956, NS-39867, and CA-21765 and by a grant from the American Lebanese and Syrian Associated Charities of Saint Jude Children's Research Hospital. Supplemental data are available on the AACR Web site.

[2] To whom requests for reprints should be addressed, at Genetics, 332 North Lauderdale Street, Memphis, TN 38105. Phone: (901) 495-2700; Fax: (901) 526-2907; E-mail: peter.mckinnon@stjude.org.

[3] The abbreviations used are: SHH, sonic hedgehog; WNT, wingless; PTC/Ptc, Patched; sFRP/sFrp, secreted Frizzled-related protein; APC, adenomatous polyposis coli; GSK-3β, glycogen synthase kinase-3β; WT, wild type; P5 and P7, postnatal days 5 and 7, respectively; EGL, external germinal layer.

animals were housed in an American Association of Laboratory Animal Care-accredited facility and were maintained in accordance with the NIH Guidelines for the Care and Use of Laboratory Animals. The Institutional Animal Care and Use Committee at St. Jude Children's Research Hospital approved all procedures for animal use. Medulloblastoma and cerebellum samples of mutant and control animals were snap frozen in nitrogen for RNA extraction or fixed for cryosectioning by transcardial perfusion with 4% buffered paraformaldehyde or by submerging the samples in 10% buffered formalin for paraffin preparation. Fixed tissues were cryoprotected in 25% buffered sucrose solution and cryosectioned at 8 μm or embedded in paraffin and sectioned at 5 μm.

Human Tissue. With the approval of the St Jude Children's Research Hospital Institutional Review Board, tumor material from 50 children ($\leq$19 years of age) undergoing surgical resection of a primary medulloblastoma was collected and snap frozen. Fixed tumor material from the same tissues was used for central pathology review to confirm the diagnosis and subtype of medulloblastoma. Frozen sections from each case were examined by light microscopy to ensure that $\geq$80% consisted of tumor. Samples were then subdivided, and RNA or protein was extracted after direct homogenization in Trizol (Invitrogen) or sonication in protein lysis buffer, respectively. The expression of individual mRNA was measured by real-time PCR (see below). ERBB2 protein expression in each tumor was determined using Western blot analysis as described (35) with the anti-ERBB2 mouse monoclonal antibody NCL-CB11 (Novacastra). Blots were reprobed with a monoclonal antibody for β-actin (Sigma Chemicals) to control for protein loading. Unsupervised hierarchical cluster analysis was performed using Pearson coefficient analysis (GeneMaths version 2.01; Applied Maths, Inc.). Direct comparisons between molecular and clinical covariables were performed using Fisher's exact test.

GeneChip Hybridization. Total RNA was extracted using Trizol (Invitrogen) according to the manufacturer's instructions. For comparative medulloblastoma analyses, tissues were obtained from $Lig4^{-/-}p53^{-/-}$ ($n = 3$), $Ptc1^{+/-}$ ($n = 2$), $Ptc1^{+/-}p53^{-/-}$ ($n = 2$), $Ink4d^{-/-}Kip1^{+/-}p53^{-/-}$ ($n = 1$), $Kip1^{-/-}p53^{-/-}$ ($n = 1$), $Ink4c^{-/-}p53^{-/-}$ ($n = 1$), and $Ink4d^{+/-}$ $Ink4c^{-/-}p53^{-/-}$ ($n = 2$), and the controls were adult WT ($n = 3$) 9 weeks of age, $p53^{-/-}$ ($n = 2$) 9 weeks of age, WT ($n = 3$, one sample pooled from three animals) at P5, and $p53^{-/-}$ ($n = 2$, with one sample pooled from three animals) at P5.

RNA quality and integrity for microarray were assessed using the Agilent 2100 Bioanalyzer (Agilent). Double-stranded cDNA from total RNA was synthesized using the SuperScript Double-Stranded cDNA Synthesis kit (Life Technologies, Inc.) and T7-dT24-DNA primer GGCCAGTGAATTGTAATACGACTCACTATAGGGAGGCGG, according to the manufacturer's instructions. Using this double-stranded cDNA as a template, a labeled antisense cRNA was synthesized with biotinylated UTP and CTP by *in vitro* transcription using the T7 RNA Transcript Labeling kit (ENZO Diagnostics, Inc.). The labeled cRNA was passed through a CHROMA SPIN-100 column (Clontech), fragmented by heating and ion-mediated hydrolysis, and then used for hybridization to murine genome MG_U74Av2 oligonucleotide arrays (Affymetrix) according to the manufacturers' instructions. After hybridization, oligonucleotide arrays were washed and stained with phycoerythrin-conjugated streptavidin (Molecular Probes). The arrays were then scanned using a laser confocal scanner (Agilent), and expression signals of each gene were calculated using Affymetrix Microarray version 4.0 software (MAS v4).

Data Analysis. Data analysis was done using GeneSpring version 5.0 software (Silicon Genetics). Initially, per-chip and per-gene normalizations were done for all Affymetrix array output data to control for variations between different analyses in intensity and difference in detection efficiency between spots within an array, using the 50th percentile of all measurements as a positive control for each sample. Background corrections were applied using the lower tenth percentile intensities as needed during normalization. Only genes marked as "Marginal" or "Present" were used for normalization. After normalization, data from each medulloblastoma sample could be compared directly to other medulloblastoma samples or control groups. These normalized values were filtered using the two-component Roche-Lorenzato model for estimating variation from control strength. Furthermore, data were restricted with a one-way ANOVA (cutoff, $P < 0.05$ in different genotypes). Finally, genes with "Present" calls in more than half of experimental samples were taken for additional statistical analyses. Using these approaches for quality control, array data with low signal intensity or genes with very low variation throughout the entire experimental groups were removed. The selected group of genes from this quality control was examined by unsupervised analysis strategies to find subgroups of genes based on similar expression patterns in an unbiased manner. K-means cluster analysis (four different groupings) and a self-organizing map (4×4-dimension grouping) identified two major patterns of expression profiles that showed either increased or decreased expression levels in the entire medulloblastoma samples compared with control groups. Supervised analyses were then used to identify up-regulated or down-regulated genes in the entire medulloblastoma compared with control arrays. A normalized value for individual genes of each medulloblastoma was compared with those of either adult or P5 control groups, and only genes with at least 2-fold difference were selected for hierarchical cluster analyses.

Real-Time PCR. Real-time PCR was done using a 7900HT Sequence Detection System (ABI) and the TaqMan One Step PCR Master Mix Reagents kit (AIB). Oligonucleotide primers and a TaqMan probe for each gene were designed using Primer Express version 2.0 software (ABI). Primer/TaqMan probe sets for murine genes were: *sFrp1* 5′-TCCTCCATGCGACAACGA (forward), 5′-TGATTTTCATCCTCAGTGCAAACT (reverse), and 5′-TGAAGTCAGAGGCCATCATTGAACATCTCTG (TaqMan probe); *Ptc2* 5′-TGGAGCCACCTTGGTACAAGA (forward), 5′-GGCGCTCAGGAAAGCATGT (reverse), and 5′-CTGGCCCTGACAGATGTGGTCCCT (TaqMan probe); *Math1* 5′-ATGCACGGGCTGAACCA (forward), 5′-TCGTTGTTGAAGGACGGGATA (reverse), and 5′-CCTTCGACCAGCTGCGCAACG (TaqMan probe); *Gli1* 5′-GCTTGGATGAAGGACCTTGTG (forward), 5′-GCTGATCCAGCCTAAGGTTCTC (reverse), and 5′-CCGGACTCTCCACGCTTCGCC (TaqMan probe); and *Jpo1* CTTTCCCTACAGGTGGGTCATT (forward), 5′-TAGGCACAGCTGACAGGCTACA (reverse), and 5′-TACTGGTGACGAAGTGACTGAGTCCCTCAC (TaqMan probe).

Primer/TaqMan probe sets for human genes were: *sFRP1* 5′-ACACGCACTGCCCTGTCA (forward), 5′-TTTGGAGCGTGGCTATGGA (reverse), and 5′-CTTGTTCTTGCAGCATTCCCGCTCC (TaqMan probe); *PTC2* 5′-ATCCTAGCTGGGAGCCTGAAG (forward), 5′-TCCCGCATCCCAGAGAGA (reverse), and 5′-TCCACTCTGGCTTCGTGCTTACTTCCA (TaqMan probe); *MATH1* 5′-CCAAATATGAGACCCTGCAGATG (forward), 5′-CCTCCGCTGGGCGTTT (reverse), and 5′-CCAAATCTACATCAACGCCTTGTCCGA (TaqMan probe); *GLI1* 5′-GGACCTGCAGACGGTTATCC (forward), 5′-AGCCTCCTGGAGATGTGCAT (reverse), and 5′-CCTCACCCAGCTCCCTCGTAGCTTTC (TaqMan probe); and *JPO1* 5′-GTGGATGGCTACATGAATGAAGAT (forward), 5′-CGGAAGGGTCACGGATGAT (reverse), and 5′-CTGCCCAGAAGCCGTCGCTCC (TaqMan probe). Real-time PCR data were analyzed using SDS version 2.0 software (ABI). Total RNA from the cerebral cortex of neonatal WT animals for murine genes and total RNA from human adult (Ambion) or fetal (Clontech) brains for human genes were used to generate standard curves for relative quantitation, and 18S rRNA assay reagents (ABI) were used as an internal standard.

Histology and *in Situ* Hybridization. Mouse paraffin sections were stained with H&E according to standard procedures. For *in situ* hybridization, medulloblastomas from $Ptc1^{+/-}p53^{-/-}$ and $Lig4^{-/-}p53^{-/-}$ as well as age-matched adult and P7 WT brains were examined. Nucleotides 247-1375 of *sFrp1* (GenBank accession U88566) and nucleotides 701-1251 of *Gli1* (GenBank accession AB025922) were generated using standard PCR methods from mouse embryonic cDNA library as a template and were cloned into pSPORT1 (Life Technologies, Inc.). The *sFrp1* primers were 5′-GGGCGGCCGCCGACGTCGCCGAGCAACATGG (forward) and 5′-CCGTCGACCACTTAAAAACAGACTGGAAGG (reverse). The *Gli1* primers were 5′-GCGGCCGCAAGCTGAAGTCAG (forward) and 5′-GTCGACCGAAGGGTGCGTCT (reverse). Full-length *Math1* (*atoh1*, GenBank accession NM_007500) was isolated using PCR and then cloned into pGEM-T Easy (Promega). Math1 primers were 5′-CTCGTCGACCAGTGCGATGTCCCGCCTGCTG (forward) and 5′-CGCGAGCTGTTGCCTTCCTAACTGGCCTCATC (reverse). IMAGE[4] clones for *Ptc1* (clone 3989319; nucleotides 3521–4281 and 3′ untranslated region) and *Ptc2* (clone 3972649; nucleotides 1891–3568 and 3′ untranslated region) were obtained from Research Genetics, Inc. *In situ* hybridization was done using sense and antisense ^{33}P riboprobes using T7, T3, or SP6 RNA polymerase (Promega), according to the manufacturer's directions.

[4] Internet address: http://est.llnl.gov/.

Cryosections were washed in 0.1 M Tris/50 mM EDTA (pH 8.0) buffer, followed by acetylation with 0.25% acetic anhydride/0.1 M triethanolamine (pH 8.0). Slides were then rinsed in 2× SSC and dehydrated in an ethanol series. Sections were hybridized at 60°C overnight in 600 mM NaCl, 10 mM Tris (pH 8.0), 0.02% Ficoll, 0.02% polyvinylpyrrolidone, 0.1% BSA, 1 mM EDTA (pH 8.0), 10% dextran sulfate, 100 μg/ml salmon sperm DNA, 50 μg/ml total yeast RNA, 50 μg/ml yeast tRNA, and 50% deionized formamide. Slides were then rinsed in 4× SSC/50% formamide, followed by washing in 2× SSC, treated with 20 μg/ml RNase A in 10 mM Tris/1 mM EDTA (pH 8.0)/500 mM NaCl to remove unbound probe, washed in 2× SSC, followed by 0.2× SSC, and then dehydrated in ethanol. The *in situ* signals were visualized using NTB2 emulsion (Kodak) according to the manufacturer's recommendations. Images were captured with a Spot digital camera (Diagnostic Instruments, Inc.) and processed using Adobe Photoshop version 7.0 software.

Radiosensitivity Analysis. Radiosensitivity experiments were done using *Ptc1*$^{+/-}$ or *Ink4c*$^{-/-}$ and their WT littermates by irradiating P5 mice with 18 Gy from a cesium irradiator (at a rate of 4.3 Gy/min). Brains were collected at 3 and 6 h postirradiation after transcardial perfusion with 4% paraformaldehyde. Two WT and two mutant P5 pups were collected at each time point. Cryosections of these brains were stained with 1% neutral red (Aldrich Chemical) in 0.1 M acetic acid (pH 4.8). Pyknotic cells present in the EGL of the first and second folia in the midsagittal and paramidsagittal sections of the cerebellum were counted using a double-blind method. The number of pyknotic cells present after irradiation was determined using the Bonferroni *t* test. Comparisons with $P < 0.05$ were considered significantly different.

RESULTS

Gene Expression Profiles of Mouse Medulloblastomas Are Similar to Early Postnatal Cerebellum. To identify genes that are deregulated during medulloblastoma development, we generated Affymetrix (U74Av2) microarray gene expression profiles from murine medulloblastomas arising spontaneously in seven different genetically altered mice. The murine medulloblastoma models used in this study were *Ptc1* haploinsufficient [*Ptc1*$^{+/-}$; medulloblastoma occurrence, ~15% (12, 13)], *Ptc1*$^{+/-}$ with inactivation of p53 [*Ptc1*$^{+/-}$*p53*$^{-/-}$; medulloblastoma occurrence, 100% (30)], and DNA ligase IV with

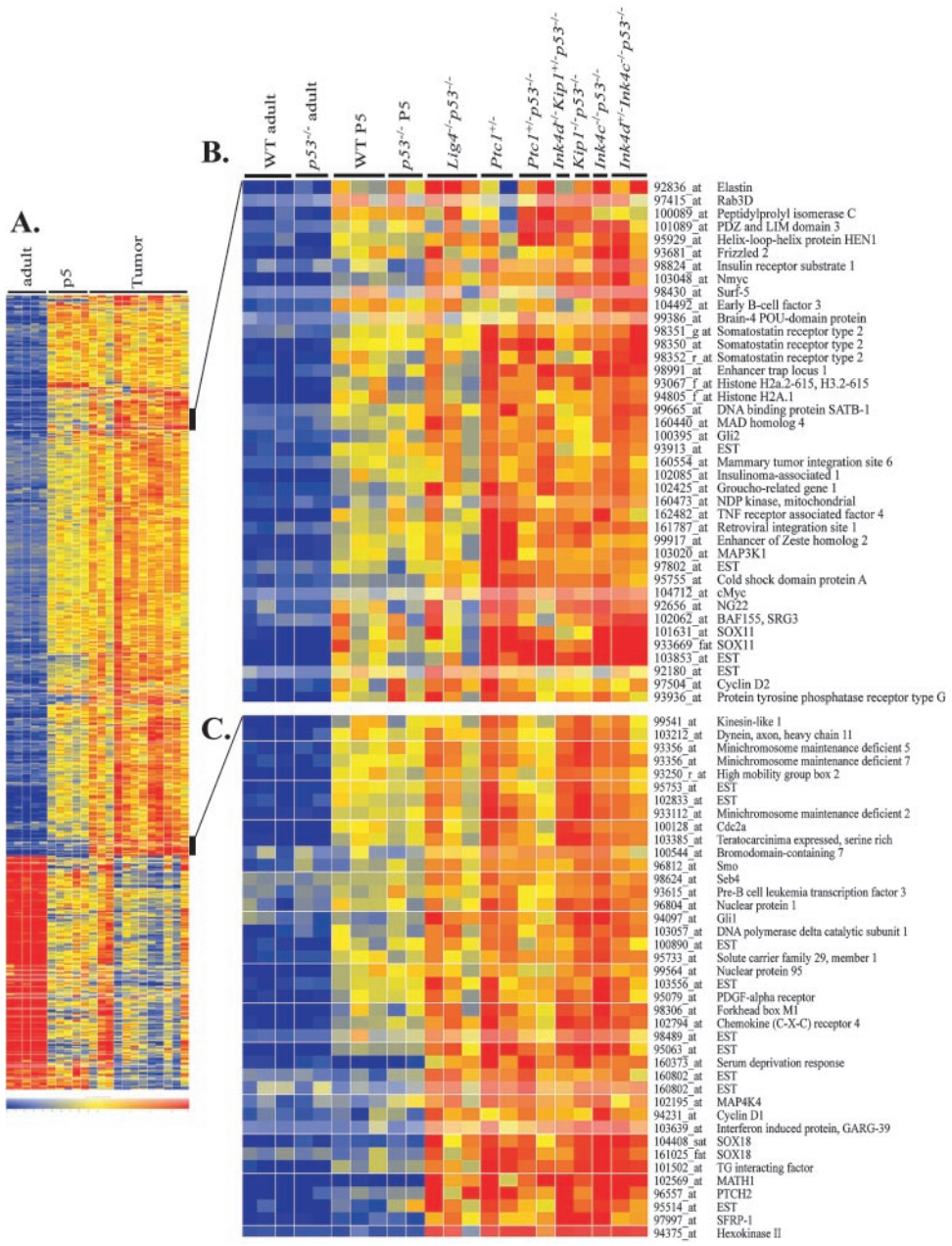

Fig. 1. Medulloblastoma gene expression is very similar to early postnatal cerebellum. Hierarchical cluster analysis of gene expression changes in the adult cerebellum compared with developing cerebellum (P5) and those from tumors derived from different mutant mice that had developed medulloblastoma is presented. *A*, 697 genes with at least 2-fold expression changes after hierarchical cluster analysis of the entire filtered data set of 3,119 genes. Colors indicate high expression (*red*) to low expression (*blue*) and correspond to relative expression changes between 0 and 2.5 of normalized values. *B*, an expanded view of the indicated section in *A*, which illustrates the similarity between developing cerebellum and each of the medulloblastomas. *C*, an expanded view of an area of *A* that contains genes that are relatively specific to the medulloblastoma samples. Medulloblastomas were obtained from the following mice: *Ptc1*$^{+/-}$, *Ptc1*$^{+/-}$*p53*$^{-/-}$, *Lig4*$^{-/-}$*p53*$^{-/-}$, *Kip1*$^{-/-}$*p53*$^{-/-}$, *Ink4d*$^{+/-}$*Ink4c*$^{-/-}$*p53*$^{-/-}$, *Ink4d*$^{-/-}$*Kip1*$^{+/-}$*p53*$^{-/-}$, and *Ink4c*$^{-/-}$*p53*$^{-/-}$. The individual gene names shown on the *right* of *B* and *C* correspond to the *rows* in the cluster.

p53 inactivation [*Lig4*$^{-/-}$*p53*$^{-/-}$; medulloblastoma occurrence, 100% (25)]. We also used medulloblastoma samples from *p53*$^{-/-}$ mice with disruption of inhibitors of cyclin-dependent kinases (*Kip1*$^{-/-}$*p53*$^{-/-}$, *Ink4d*$^{+/-}$*Ink4c*$^{-/-}$*p53*$^{-/-}$, *Ink4d*$^{-/-}$*Kip1*$^{+/-}$*p53*$^{-/-}$, and *Ink4c*$^{-/-}$*p53*$^{-/-}$) in which medulloblastoma occurs with an incidence of 5–15% by 5 months of age.[5] Inhibitors of cyclin-dependent kinases can regulate Rb function and may act in this manner to promote transformation, because disabling the Rb and p53 pathways leads to medulloblastoma (31). However, although p53-null mice are cancer prone, they rarely develop medulloblastoma (36–38). Morphologically, the mouse tumors resemble the "classic" subtype of human medulloblastoma, except *Kip1*$^{-/-}$*p53*$^{-/-}$ medulloblastomas, which resembled the large-cell anaplastic subtype. All mouse medulloblastomas analyzed were characterized by high proliferation (Ki67 immunostaining) and apoptosis (terminal deoxynucleotidyl transferase-mediated nick end labeling-positive cells) and immunoreactivity toward synaptophysin (12, 25).

Initial data analysis comparing medulloblastoma and age-matched control cerebellum showed substantial differences in gene expression between 9-week-old tissue from WT or p53-null mice compared with the medulloblastoma samples. Because medulloblastoma may derive from granule cell precursors (2), we reasoned that a more appropriate control tissue would be the developing cerebellum. The mouse cerebellum undergoes a period of postnatal neurogenesis until 3 weeks of age, whereby granule cells that are generated in an EGL migrate inward radially, undergoing differentiation to form the internal granule cell population (39). Therefore, we tested P5 cerebellum, which contains a substantial EGL, as a potential control tissue.

We compared gene expression between medulloblastoma, P5 cerebellum, and adult cerebellum and included genes with at least 2-fold changes for hierarchical cluster analysis. We found that the overall gene expression profile of P5 cerebellum was very similar to that of medulloblastoma (Fig. 1*A*). An expanded view of select regions of the cluster analysis from Fig. 1*A* is shown in Fig. 1, *B* and *C*, and underscores the similarity in gene expression between the P5 cerebellum and the medulloblastomas. These results were obtained after normalization of the raw data to remove background noise (see "Materials and Methods"); values were filtered to eliminate nonsignificant signals compared with control signals and further sorted using a one-way ANOVA (cutoff was $P < 0.05$), and genes with Present calls in more than one-half of the samples were used in the final analysis. Thereby, data with low signal intensity or genes with very low variation throughout the entire sample set were removed; 3,119 genes passed the above criteria and were selected from 12,488 total genes and expressed sequence tags present on the Affymetrix GeneChips for each sample included in this study. Of the 3,119 genes analyzed, 494 genes showed increased expression, and 203 genes showed decreased expression in the P5 cerebellum and medulloblastoma samples compared with adult 9-week-old tissue.[6] Thus, gene expression profiles in tumors from the mouse models of medulloblastoma under study here are similar to those of the developing cerebellum but are very different from age-matched controls. These data further strengthen the notion of medulloblastoma arising as a derivative of the external granule cell population of the cerebellum.

Medulloblastoma-specific Genes Are Up-Regulated in All Mouse Tumors Independent of Genetic Background. Although medulloblastoma gene expression profiles were very similar to those of P5 cerebellum, significant gene expression differences were observed between these two tissues (Fig. 1*C*). To more thoroughly assess this cohort of genes and to identify those that are medulloblastoma specific, we reanalyzed our filtered data set to select those that averaged 2-fold differences between the medulloblastoma samples and normal tissue controls (both P5 and adult cerebellum). This analysis identified a group of 57 genes that showed increased expression in all tumor samples compared with adult and P5 controls, and 26 genes showed decreased gene expression (Fig. 2). Because this group contained genes that showed p53-specific changes in expression, we further refined this group to identify those that are specifically up-regulated in medulloblastoma independently of p53. We compared medulloblastoma gene expression to normal cerebellum (adult and

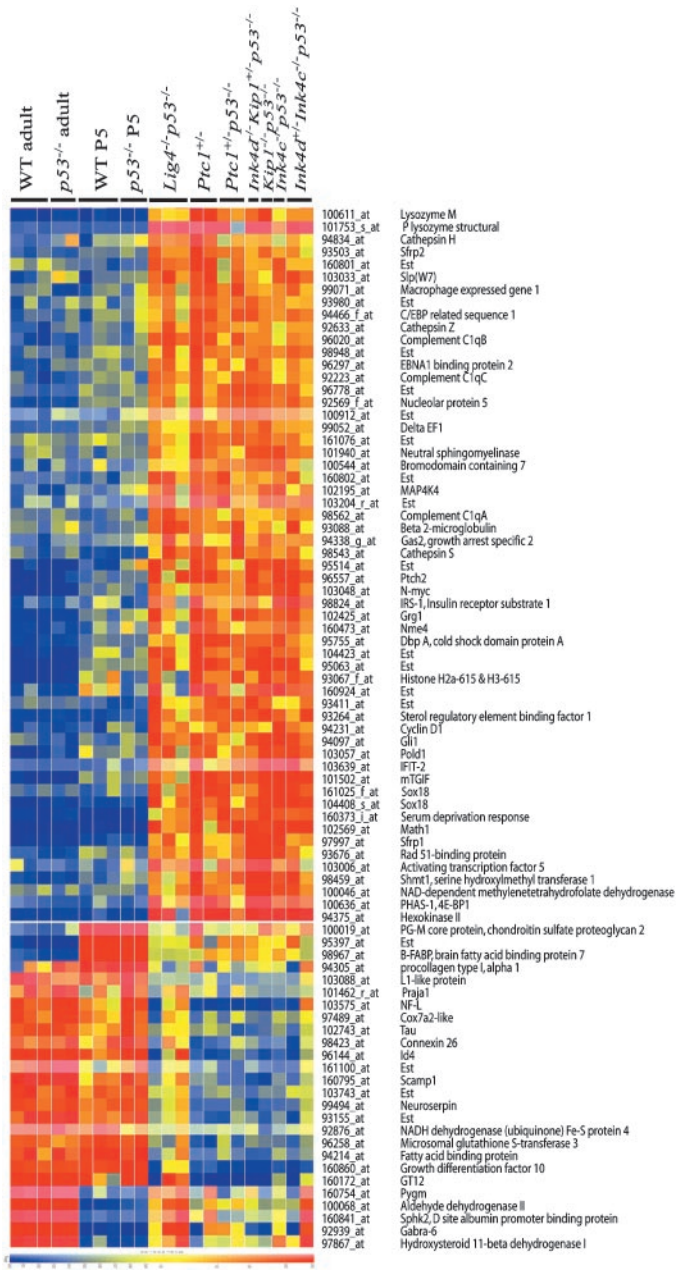

Fig. 2. Gene expression changes in medulloblastomas. Hierarchical cluster analysis of gene expression changes specific to medulloblastoma compared with developing (P5) and adult cerebellum is shown. Genes included in this analysis show an average 2-fold up-regulation in all of the tumors compared with normal and *p53*$^{-/-}$ tissues (adult and P5 cerebellum). Colors indicate high expression (*red*) to low expression (*blue*) and correspond to relative expression changes of between 0 and 2.5 of normalized values. Medulloblastomas were obtained from the following mice: *Ptc1*$^{+/-}$, *Ptc1*$^{+/-}$*p53*$^{-/-}$, *Lig4*$^{-/-}$*p53*$^{-/-}$, *Kip1*$^{-/-}$*p53*$^{-/-}$, *Ink4d*$^{+/-}$*Ink4c*$^{-/-}$*p53*$^{-/-}$, *Ink4d*$^{-/-}$*Kip1*$^{+/-}$*p53*$^{-/-}$, and *Ink4c*$^{-/-}$*p53*$^{-/-}$. Individual gene names corresponding to the *rows* in the cluster are shown on the *right*.

[5] F. Zindy and M. F. Roussel, manuscript in preparation.

[6] A complete list of these 697 genes is presented as Supplementary data, Fig. 1*S*.

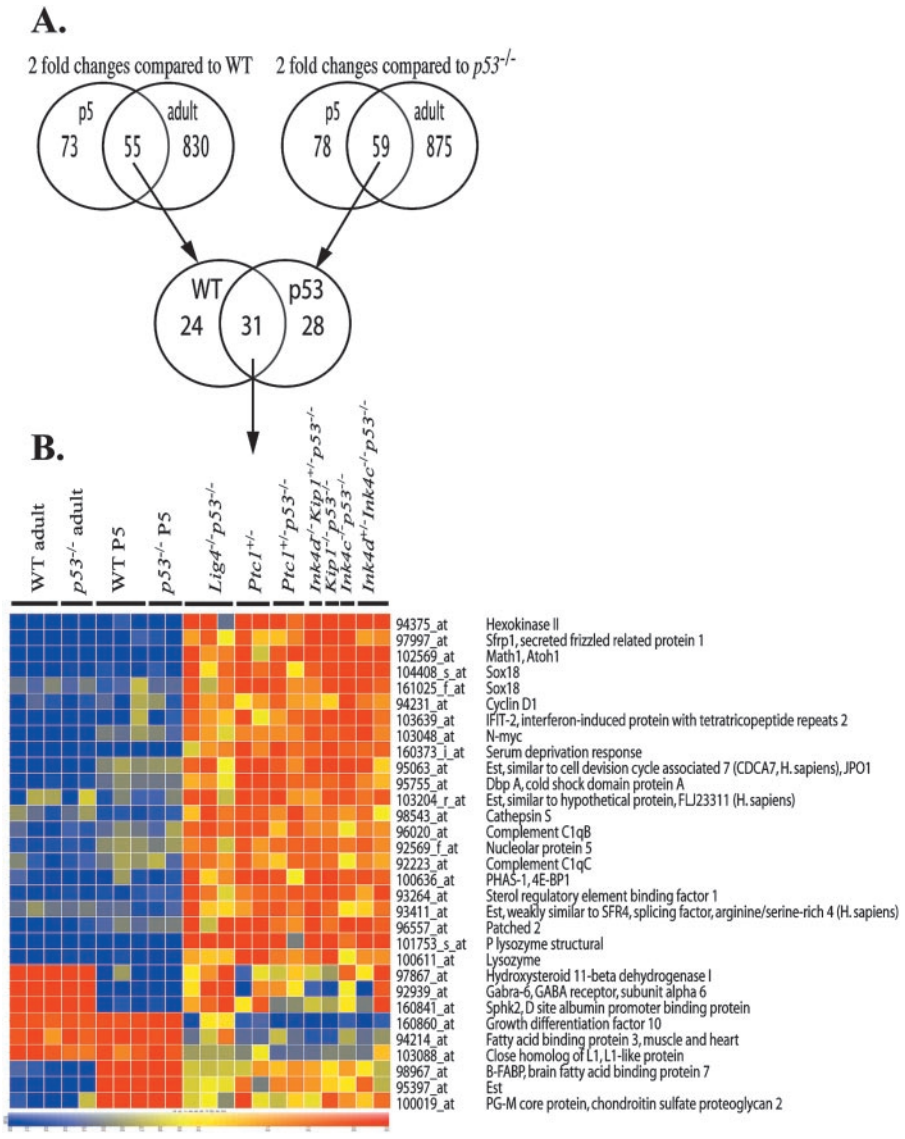

Fig. 3. Medulloblastoma-specific gene expression. Specific gene changes in the medulloblastoma occurred for 31 genes that were not altered in expression in either developing or adult WT or $p53^{-/-}$ cerebellum. *A*, the total number of differences at 2-fold or greater between all medulloblastomas and WT tissues are indicated in the Venn diagrams; a common group of 55 genes was changed in the medulloblastoma, compared with 73 between medulloblastoma and P5 tissue and 830 compared with adult tissue. For $p53^{-/-}$ tissues, there were 875 differences to adult and 78 differences to P5. Of these medulloblastoma-specific changes, 31 genes changed independently of p53 status. *B*, hierarchical cluster analysis showing all 31 gene expression changes occurring in medulloblastomas. Medulloblastomas were obtained from the following mice: $Ptc1^{+/-}$, $Ptc1^{+/-}p53^{-/-}$, $Lig4^{-/-}p53^{-/-}$, $Kip1^{-/-}p53^{-/-}$, $Ink4d^{+/-}Ink4c^{-/-}p53^{-/-}$, $Ink4d^{-/-}Kip1^{+/-}p53^{-/-}$, and $Ink4c^{-/-}p53^{-/-}$. Colors indicate high expression (*red*) to low expression (*blue*) and correspond to relative expression changes between 0 and 2.5 of normalized values. Individual gene names corresponding to the *rows* in the cluster are shown on the *right*.

P5) and then, independently, to $p53^{-/-}$ tissues (adult and P5) to generate two separate gene lists (Fig. 3*A*). We excluded genes from this list that showed any variation in expression below 2-fold changes between control and tumor groups, further reducing the size of the gene list. Notably, 55 genes were differentially regulated and specific to the medulloblastomas compared with WT cerebellum (all of these appear in the gene list of Fig. 2), whereas in the $p53^{-/-}$ tissue we identified 59 genes that were differentially regulated. Within these two lists were an overlapping group of 30 genes, the expression of which was altered in the medulloblastoma compared with both WT and $p53^{-/-}$ tissue (Fig. 3*B*). Of this group, there were 21 unique genes (*Sox18* appeared twice) that were significantly up-regulated and 9 genes that were down-regulated in all of the tumors. Analysis of gene expression between medulloblastoma samples did not identify any significant genotype-specific patterns.

Thus, the use of appropriate control tissue (P5 cerebellum) has resulted in the identification of a small cohort of genes, the expression of which is selectively up-regulated in medulloblastoma, suggesting an important role in this tumor. Importantly, some of the genes we identified have already been strongly linked to medulloblastoma, including *Gli1* and N-*Myc*, suggesting that our analysis has reliably identified genes that are meaningful for medulloblastoma. However, a number of genes that have not been implicated previously in medulloblastoma stood out from this analysis. These include *Ptc2* and *sFrp1*, which are notable for their connection to cerebellar growth regulation and to pathways disrupted in medulloblastoma. Other genes identified in this analysis suggest roles associated with cell growth and metabolism. For example, *Phas1*, *hexokinase II*, and *cyclin D1* are involved in cellular proliferation, whereas genes such as *lysozyme* and *cathepsin* are involved in protein turnover, and *Sox18* is involved in vascular development (40). The selective up-regulation of these genes, and not others involved in general cellular metabolism, suggests they are particularly relevant to medulloblastoma proliferation. Most down-regulated genes in the medulloblastoma samples were involved in normal cerebellar development, such as γ-aminobutyric acid receptor subunit α6, which is associated with mature granule cells (41).

Medulloblastoma-specific Genes Are Highly Expressed in Tumor Tissue and Are Present in Immature Proliferative Granule Cells. We confirmed the array data using real-time PCR to measure expression of representative genes identified as up-regulated in the different medulloblastomas. We selected these genes for further analysis because they were linked to medulloblastoma or to pathways important for cerebellar development. Real-time PCR analysis using

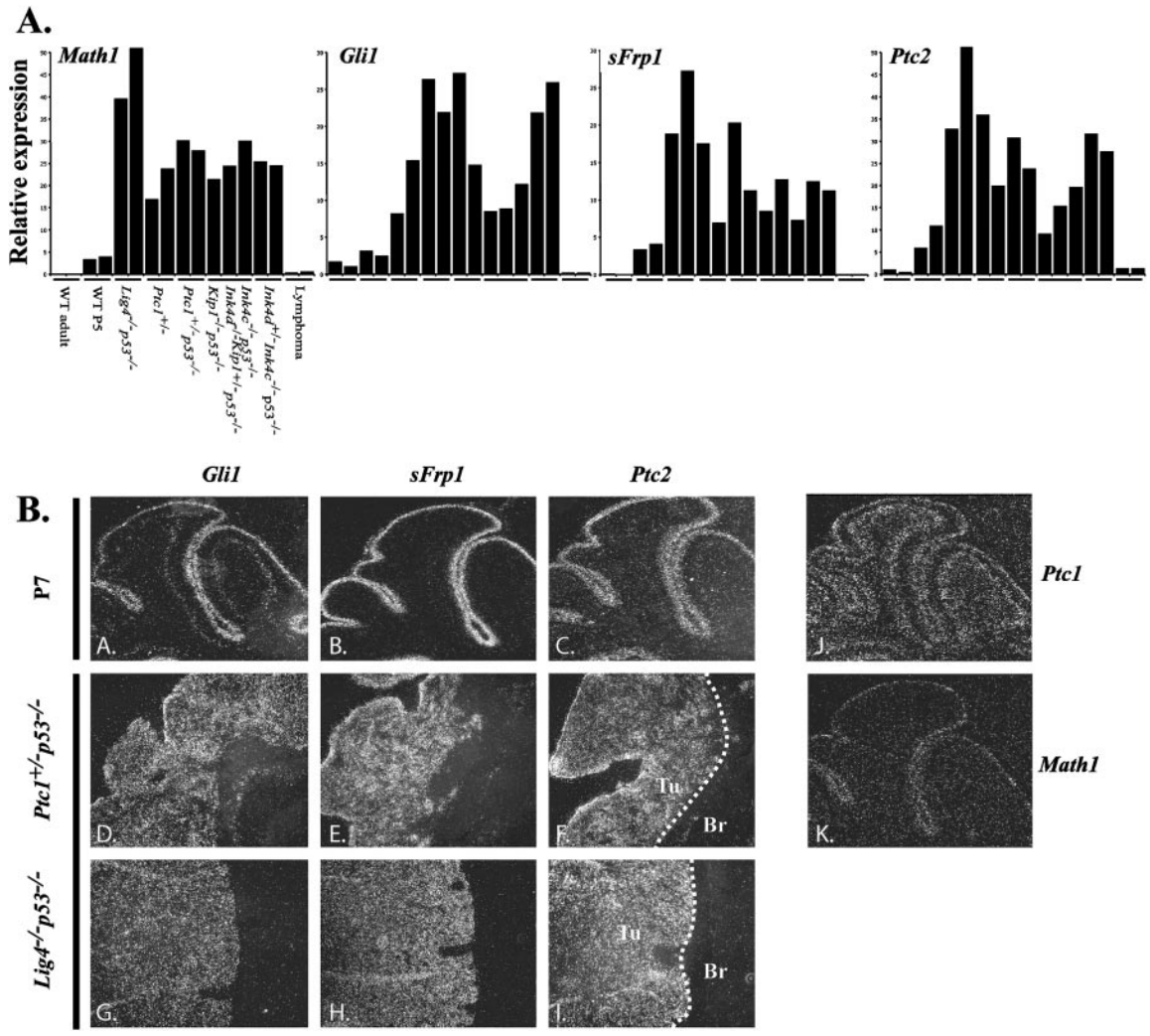

Fig. 4. Real-time PCR and *in situ* analysis of medulloblastoma-specific genes. *A*, real-time PCR was used to determine relative mRNA expression levels in each of the medulloblastomas compared with WT age-matched cerebellum and P5 developing cerebellum. Lymphoma from $Lig4^{-/-}p53^{-/-}$ mice was also used as a nonneural tumor control. 18S rRNA was used as an internal standard, and neonatal brain RNA was used as a PCR control for relative expression. Medulloblastomas are from the following mice: $Ptc1^{+/-}$, $Ptc1^{+/-}p53^{-/-}$, $Lig4^{-/-}p53^{-/-}$, $Kip1^{-/-}p53^{-/-}$, $Ink4d^{+/-}Ink4c^{-/-}p53^{-/-}$, $Ink4d^{-/-}Kip1^{+/-}p53^{-/-}$, and $Ink4c^{-/-}p53^{-/-}$. Expression scales are arbitrary and reflect relative expression between the tumors and controls for the particular gene of interest. PCR was done using TaqMan probes for the following genes: *Math1*, *Gli1*, *sFrp1*, and *Ptc2*. *B*, analysis of transcript localization using *in situ* hybridization analysis was done with antisense ^{33}P riboprobes for *Gli1*, *sFrp1*, and *Ptc2* on cryosections of developing WT P7 cerebellum (*A–C*, *J*, and *K*) or medulloblastoma and adult brain from $Ptc1^{+/-}p53^{-/-}$ and $Lig4^{-/-}p53^{-/-}$ mice (*D–I*). For comparative analysis, *in situ* hybridization of *Math1* and *Ptc1* were done on P7 cerebellum (*J* and *K*). *Dashed lines* in *F* and *I* demarcate medulloblastoma (*Tu*) and brain (*Br*).

TaqMan probes confirmed that high levels of expression of *sFrp1*, *Ptc2*, *Math1*, *Gli1*, and the Myc-responsive target *JPO1* (42) occurred in all of the medulloblastoma samples but not in WT adult or another tumor type, pro-B-cell lymphoma, also common in $Lig4^{-/-}p53^{-/-}$ animals (Ref. 43; Fig. 4*A*). Consistent with the array data, a number of other genes analyzed by real-time PCR, such as *Gli3* and *Ptc1*, did not show differential expression in the medulloblastoma samples (Ref. 25 and data not shown).

To assess tissue specificity of gene expression, we used *in situ* hybridization and detected *sFrp1*, *Ptc2*, and *Gli1* expression in the EGL of the developing P7 cerebellum and at high levels throughout the medulloblastoma but not in adult brain tissue (Fig. 4*B*). The hybridization signal in the EGL at P7 corresponds to the outer proliferative matrix layer rather than the premigratory mantle zone, indicating that expression of these genes is restricted to regions of cellular proliferation. *In situ* hybridization analysis of *Ptc1*, for comparison to *Ptc2*, and *Math1* as a marker for proliferative EGL cells, is also shown (Fig. 4, *J* and *K*). *Ptc2* expression was more restricted than *Ptc1* and was confined to the proliferative region of the EGL, suggesting a selective involvement of *Ptc2* in proliferative populations of the EGL. In all cases described above, sense probes showed no hybridization signal (data not shown). Thus, these genes are present in the proliferative cells of the EGL and at high levels in medulloblastoma, supporting a role in tumor proliferation.

Genetic Predisposition to Medulloblastomas and the Susceptibility to Genotoxic Stress. It is intriguing that a variety of different genetic backgrounds predispose to medulloblastomas with similar histology and gene expression profiles. Therefore, we questioned possible connections that could account for the similar gene expression profiles. The loss of one allele of *Ptc1* has been shown to predispose to radiosensitivity during development (28, 29), and *Ptc1* has been implicated in the DNA damage response via interaction with phosphorylated cyclin B (44). Furthermore, tumor development in $Ptc1^{+/-}$ mice is accelerated after ionizing radiation or on a $p53^{-/-}$ genetic background (30). Therefore, in some scenarios *Ptc1* deficiency predisposes to genotoxic stress, and similar to the $Lig4^{-/-}$ $p53^{-/-}$ mice, this may be important for the development of medulloblastoma. There is also substantial evidence that genotoxic stress

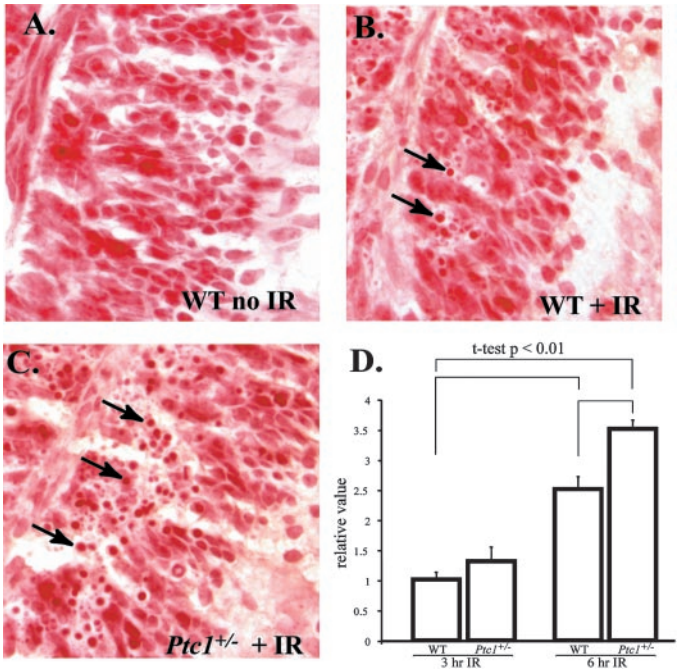

Fig. 5. $Ptc1^{+/-}$ developing cerebellum is hypersensitive to genotoxic stress-induced apoptosis. $Ptc1^{+/-}$ P5 cerebellum is significantly ($P < 0.01$) more sensitive to genotoxic stress compared with WT P5 cerebellum at 3 and 6 h after irradiation (*IR*). *A* is a P5 WT cerebellar EGL with no irradiation. *B* is WT, and *C* is $Ptc1^{+/-}$ EGL 6 h after irradiation. *Arrows*, pyknotic nuclei that indicate apoptotic cells. *D*, a quantitative representation of comparative radiation-induced apoptosis. *Bars*, SE.

features prominently in the developing nervous system, particularly the cerebellum (25, 45). Thus, to establish links between the different medulloblastoma models that could account for similar gene expression profiles, we examined the susceptibility of early postnatal developing $Ptc1^{+/-}$ and $Ink4c^{-/-}$ cerebellum to the effects of DNA damage induced by ionizing radiation. There were significantly more pyknotic nuclei present in the EGL of $Ptc1^{+/-}$ mice after 18 Gy of ionizing radiation compared with WT ($P < 0.01$), as indicated by *arrows* in Fig. 5. Quantitation of pyknotic nuclei in the $Ptc1^{+/-}$ EGL revealed a 20% increase in radiation-induced apoptosis after radiation (Fig. 5*D*). This suggests that *Ptc1* haploinsufficiency increases susceptibility to genotoxic stress in the developing cerebellum. The predisposition to medulloblastoma observed in $Ptc1^{+/-}$ and $Lig4^{-/-}$ mice may therefore involve inappropriate responses to genotoxic stress in granule neuron precursors within the EGL. However, analysis of $Ink4c^{-/-}$ mice did not show any unusual sensitivity to genotoxic stress via this apoptosis assay ($P < 0.09$; data not shown). The substantially lower rate of medulloblastoma occurrence in the $Ink4c^{-/-}p53^{-/-}$ mice compared with the $Lig4^{-/-}p53^{-/-}$ and $Ptc1^{+/-}p53^{-/-}$ mice (100% incidence) possibly reflects a lower susceptibility to endogenous genotoxic stress.

Mouse Medulloblastoma-specific Genes Are Up-Regulated in a Distinct Subgroup of Human Medulloblastomas. To gauge the clinical relevance of the genes up-regulated in the mouse medulloblastoma, we determined the expression of *sFRP1*, *PTC2*, *GLI1*, *MATH1*, and *JPO1* in a large cohort ($n = 50$) of human pediatric medulloblastomas. Unsupervised hierarchical cluster analysis of real-time PCR expression values for these genes identified a distinct subgroup of human tumors, which we termed group B (16 of 50; 32%), in which these genes were up-regulated (all $P < 0.0001$; Fig. 6). Group B patients also had a significantly greater incidence of *ERBB2* oncogene expression ($P < 0.05$). ERBB2 expression has been shown previously to associate with increased mitotic index, metastasis, and poor clinical outcome in medulloblastoma (46). Indeed, group B patients had a shorter 5-year survival rate (54% ± 14.3) compared with group A patients (70% ± 8.5), although this difference in survival did not reach statistical significance. Analysis of $Ptc1^{+/-}p53^{-/-}$ and $Lig4^{-/-}p53^{-/-}$ mouse tumors by Western blot analysis and immunohistochemistry demonstrated that these also express high levels of murine Erbb2, while the levels are very low in developing cerebellum (data not shown). Therefore, the genetic mouse models of medulloblastoma analyzed in the current study may recapitulate some of the molecular characteristics of the aggressive ERBB2-expressing form of human medulloblastoma. The distribution of other clinical parameters including patient age and metastatic stage were not significantly different between groups A and B; however, there was a tendency for group B tumors to display desmoplastic morphology ($P < 0.06$). Expression of the myc-responsive gene *JPO1* was not linked to *sFRP1*, *PTC2*, *GLI1*, or *MATH1*. The general expression of *JPO1* may be related to high c- or N-MYC expression in most of the human tumors (data not shown). Analysis of more human tumors will establish whether the gene expression pattern observed among group B tumors correlates with ERBB2 expression and poor-outcome medulloblastoma and whether this pattern is associated with specific tumor histopathology.

DISCUSSION

Gene expression microarray analyses of several different mouse medulloblastomas revealed a characteristic common molecular fingerprint. Additionally, the remarkable similarity of medulloblastoma gene expression profiles to those of early postnatal cerebellum argues strongly that the germinal layer in this tissue harbors the precursor cells for medulloblastoma. Finally, our mouse data have been used to identify a subgroup of genes that are commonly deregulated in human medulloblastomas, underscoring the relevance of the mouse for insights into human tumor biology.

In humans, it is generally problematic to identify and obtain appropriate normal tissue for comparative analysis with tumors. The lack of correct control tissue hampers identification of gene expression changes relevant to transformation. Therefore, in lieu of normal controls, microarray approaches to understanding human tumors often compare features that are clearly defined between tumor groups, such as response to chemotherapy, survival, metastasis, or disease reoccurrence (47–52). Although these studies are valuable, they are unlikely to identify key genetic changes that may be causative for tumorigenesis. Notably, with the exception of N-*MYC* and *GLI*, analysis of human medulloblastoma (52) did not feature the same set of genes as we identified in our study, probably because of an absence of appropriate normal tissue. Using developing cerebellum as a normal tissue control, we identified a small number of genes that are highly up-regulated in medulloblastoma. This previously unrecognized cohort of 20 genes was coordinately up-regulated in all mouse medulloblastomas studied and, therefore, define a characteristic fingerprint for these tumors. Although these genes may also be expressed in proliferating EGL, their inclusion in this list is not simply a reflection of medulloblastoma as an expanding EGL. For example, whereas ~670 genes showed similar expression between the P5 cerebellum and the tumors (Fig. 1), only 21 genes were exclusively up-regulated in medulloblastoma compared with P5 tissue, suggesting that they may have specific relevance to the tumorigenic process.

Of particular note, we identified the overexpression of select members of the SHH and WNT pathways, *PTC2* and *sFRP1*, in both human and mouse tumors. Although disruption of these pathways can be causal in medulloblastoma (2), *PTC2* and *sFRP1* have not been implicated previously in this tumor. However, although overexpres-

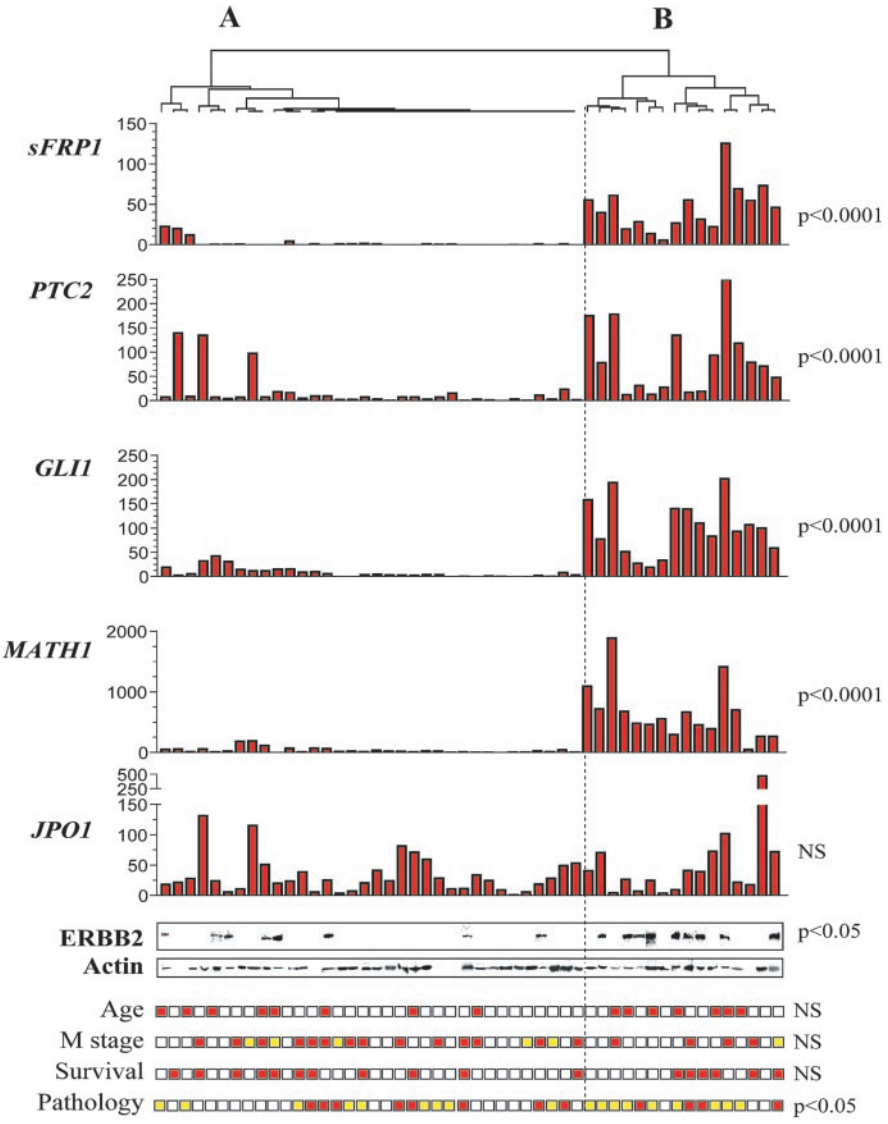

Fig. 6. Comparative gene expression in human medulloblastoma. Real-time PCR was used to determine the relative expression levels of *SFRP1, PTC2, GLI1, MATH1,* and *JPO1* in a number of human medulloblastomas. Using *SFRP1, PTC2, GLI1, MATH1,* and *JPO1* expression values as covariables, unsupervised hierarchical cluster analysis identified two distinct subgroups among the 50 tumor samples (*A* and *B*, separated by a *dashed vertical line*). Group B included 16 samples that coexpressed high levels of *SFRP1, PTC2, GLI1,* and *MATH1*. These genes were expressed at a low level in group A tumors. *JPO1* expression demonstrated no specific pattern among tumor samples. ERBB2 protein expression for each tumor was determined by Western blot analysis. Actin expression was used as a protein loading control. The results are shown immediately *below* those of the real-time PCR analyses for the corresponding tumor. Expression of ERBB2 occurred with greater frequency among group B patients (Fisher's exact test, $P < 0.05$). *Colored boxes* represent various clinical parameters for each tumor including: *Age* (*red box*, <3 years; □, ≥3 years); metastatic (*M*) stage (□, M0; *yellow box*, M1–2; *red box*, M3); *Survival* (*red box*, dead of disease; □, alive and disease free); Pathology (□, classic; *yellow box*, desmoplastic; *red box*, large cell anaplastic). *NS*, not significant.

sion of *PTC2* has been associated with basal cell carcinoma (53), mutations in *PTC2* are not commonly associated with medulloblastoma (49). Given the connection between *PTC1* and medulloblastoma, and the sequence (and probably functional) similarity between PTC1 and PTC2 (54), abnormally high *PTC2* expression in medulloblastoma may reflect disruption of coordinated functions between PTC1 and PTC2 during SHH signaling. Generation of a *Ptc2*-null mouse will be valuable for investigating the role of this protein during tumorigenesis and cerebellar development. Recently, both *sFrp1* and *Ptc2* have been shown to be targets of SHH signaling (55); although in this case SHH promoted up-regulation of *Ptc2* but repression of *sFrp1*, perhaps reflecting differences in biological context between cell lines and tumors. Moreover, in proliferating granule neuron precursors, *sFrp1* and *Ptc2* were detected by *in situ* hybridization, suggesting that these genes are functionally relevant in this proliferating population (Fig. 4). Except for an ability of sFrp1 to bind directly to Wnt and the modulation of metanephric development in a cell culture system (56, 57), little functional data are available for the secreted Frizzled-related genes, although modulation of the Wnt pathway is likely to have substantial effects upon cerebellar development (see the "Introduction").

In addition to *sFrp1* and *Ptc2*, other genes identified in our analyses, such as *Gli1*, N-*Myc*, and *cyclin D1*, are functionally important for cerebellar development and further point to a persistent activation of the SHH pathway (58–61). N-*Myc* has been shown to control cell cycle progression of cerebellar granule neuron precursor cells after SHH stimulation (59), and N-*Myc*-null cerebellum is markedly reduced in size because of attenuation of proliferation linked to a failure to suppresses $p18^{Ink4c}$ and $p27^{Kip1}$ (61). Thus, overexpression of N-Myc likely provides a significant proliferative advantage to cerebellar granule cells. Previous work reported N-*MYC* up-regulation as a feature of desmoplastic medulloblastoma (52), although our data suggest a more general N-*MYC* association with this disease. Furthermore, *cyclin D* is directly linked to growth promotion by SHH (58), and inactivation of *cyclin D1* (and *cyclin D2*) in the mouse markedly affects normal cerebellar development and function (60). Thus, our data argue that the SHH pathway is perturbed in all mouse medulloblastomas studied, despite the different genetic lesions underpinning these tumors. Importantly, the readout of this pathway is context dependent because SHH stimulation *in vitro* using either cerebellar granule neurons or mesenchymal cells leads to a different spectrum of gene expression changes than those we observed in medulloblastoma (55, 62). Therefore, *in vivo* analysis of cerebellar signaling provides important additional insights into the biology of the SHH pathway.

Many of the mutant mice used in this study are p53 deficient. p53 is a transcription factor important for control of cell proliferation and

apoptosis, and mutation of *p53* is an important cooperating event in carcinogenesis (63). Published data support a strong connection between *p53* mutations in human medulloblastoma; the results of several studies suggest an incidence of ~10% (64–69). Additionally, high p53 levels are found in up to 40% of medulloblastomas, implying that some aspect of p53 signaling is dysfunctional, because elevated levels of p53 exist without the tumor cells undergoing proliferative arrest or apoptosis (70, 71). For comparison, *PTC1* mutations have been reported to occur at a similar frequency of 9.5% (72–76). Thus, mutation of p53 represents one of the more frequent genetic alterations reported to occur in human medulloblastoma. All of the mouse models described here, with the exception of $Ptc1^{+/-}$ mice, harbor germ-line mutations in *p53*, further underscoring the relevance of p53 deficiency to this disease. Interestingly, the gene expression patterns observed in the $Ptc1^{+/-}$ tumors are remarkably similar to those in $Ptc1^{+/-}p53^{-/-}$ tumors. As has been suggested for lymphoma (77), defective p53 responses may attenuate apoptosis, subsequently increasing the probability that granule neuron precursor cells will develop mutations that promote deregulated growth leading to medulloblastoma. Because cerebellar granule cells are the most abundant neuronal cell in the nervous system, they are a large target for the stochastic acquisition of mutations.

The importance of the mouse data for understanding human medulloblastoma is highlighted by the identification of a similar subset of genes coordinately deregulated in human tumors (16 of 50; 32%) including *sFRP1* and *PTC2*. Thus, the mouse models of medulloblastoma studied in this report share molecular characteristics with a significant proportion of human medulloblastomas and therefore provide important models of this disease. This unique *sFRP1* expression signature occurs despite up-regulation of either c- or N-*MYC* in most of the human tumors,[7] suggesting that MYC overexpression is a general growth-promoting activity, rather than a specific primary event. The increase in *MYC* expression also probably accounts for the relatively high *JPO1* expression throughout the human medulloblastoma samples. It will be important to identify what distinguishes the *sFRP1*-expressing tumors from the other tumors used in our analysis. If this group (Fig. 6, group A) does not involve alterations in the SHH pathway, then it will be important to determine which other pathways are perturbed in this subset of medulloblastomas. A significantly greater proportion of the *sFRP1*-positive tumors expressed high levels of ERBB2 protein. Because high *sFRP1* expressing tumors correlate with increased ERBB2 and because this is linked to a poor clinical outcome in medulloblastoma patients (35), it will be important to increase the human tumor sample size to better determine correlates with other tumor features such as prognosis and metastasis. The molecular fingerprint for medulloblastoma described in this report may help to define a unique subtype of tumor for which particular therapies may be more appropriate.

ACKNOWLEDGMENTS

We thank Dr. Suzanne Baker for discussions and comments on the manuscript.

REFERENCES

1. Giangaspero, F., Bigner, S. H., Kleihues, P., Pietsch, T., and Trojanowski, J. Q. Medulloblastoma. *In:* P. Kleihues and W. K. Cavenee (eds.), Pathology and Genetics of Tumours of the Nervous System, pp. 129–137. Lyons: IARC Press, 2000.
2. Wechsler-Reya, R., and Scott, M. P. The developmental biology of brain tumors. Annu. Rev. Neurosci., *24:* 385–428, 2001.
3. Gilbertson, R. Paediatric embryonic brain tumours. Biological and clinical relevance of molecular genetic abnormalities. Eur. J. Cancer, *38:* 675–685, 2002.
4. McMahon, A. P., Ingham, P. W., and Tabin, C. J. Developmental roles and clinical significance of hedgehog signaling. Curr. Top. Dev. Biol., *53:* 1–114, 2003.
5. Moon, R. T., Bowerman, B., Boutros, M., and Perrimon, N. The promise and perils of Wnt signaling through β-catenin. Science (Wash. DC), *296:* 1644–1646, 2002.
6. Marti, E., and Bovolenta, P. Sonic hedgehog in CNS development: one signal, multiple outputs. Trends Neurosci., *25:* 89–96, 2002.
7. Kalderon, D. Similarities between the Hedgehog and Wnt signaling pathways. Trends Cell Biol., *12:* 523–531, 2002.
8. Hahn, H., Wicking, C., Zaphiropoulous, P. G., Gailani, M. R., Shanley, S., Chidambaram, A., Vorechovsky, I., Holmberg, E., Unden, A. B., Gillies, S., *et al.* Mutations of the human homolog of Drosophila *patched* in the nevoid basal cell carcinoma syndrome. Cell, *85:* 841–851, 1996.
9. Taylor, M. D., Liu, L., Raffel, C., Hui, C. C., Mainprize, T. G., Zhang, X., Agatep, R., Chiappa, S., Gao, L., Lowrance, A., *et al.* Mutations in *SUFU* predispose to medulloblastoma. Nat. Genet., *31:* 306–310, 2002.
10. Toftgard, R. Hedgehog signalling in cancer. Cell. Mol. Life Sci., *57:* 1720–1731, 2000.
11. Zurawel, R. H., Allen, C., Wechsler-Reya, R., Scott, M. P., and Raffel, C. Evidence that haploinsufficiency of *Ptch* leads to medulloblastoma in mice. Genes Chromosomes Cancer, *28:* 77–81, 2000.
12. Wetmore, C., Eberhart, D. E., and Curran, T. The normal *patched* allele is expressed in medulloblastomas from mice with heterozygous germ-line mutation of *patched*. Cancer Res., *60:* 2239–2246, 2000.
13. Goodrich, L. V., Milenkovic, L., Higgins, K. M., and Scott, M. P. Altered neural cell fates and medulloblastoma in mouse *patched* mutants. Science (Wash. DC), *277:* 1109–1113, 1997.
14. Fearnhead, N. S., Britton, M. P., and Bodmer, W. F. The ABC of *APC*. Hum. Mol. Genet., *10:* 721–733, 2001.
15. Bienz, M. The subcellular destinations of APC proteins. Nat. Rev. Mol. Cell Biol., *3:* 328–338, 2002.
16. Novak, A., and Dedhar, S. Signaling through β-catenin and Lef/Tcf. Cell. Mol. Life Sci., *56:* 523–537, 1999.
17. Dahmen, R. P., Koch, A., Denkhaus, D., Tonn, J. C., Sorensen, N., Berthold, F., Behrens, J., Birchmeier, W., Wiestler, O. D., and Pietsch, T. Deletions of *AXIN1*, a component of the WNT/wingless pathway, in sporadic medulloblastomas. Cancer Res., *61:* 7039–7043, 2001.
18. Huang, H., Mahler-Araujo, B. M., Sankila, A., Chimelli, L., Yonekawa, Y., Kleihues, P., and Ohgaki, H. *APC* mutations in sporadic medulloblastomas. Am. J. Pathol., *156:* 433–437, 2000.
19. Koch, A., Waha, A., Tonn, J. C., Sorensen, N., Berthold, F., Wolter, M., Reifenberger, J., Hartmann, W., Friedl, W., Reifenberger, G., Wiestler, O. D., and Pietsch, T. Somatic mutations of WNT/wingless signaling pathway components in primitive neuroectodermal tumors. Int. J. Cancer, *93:* 445–449, 2001.
20. Eberhart, C. G., Tihan, T., and Burger, P. C. Nuclear localization and mutation of β-catenin in medulloblastomas. J. Neuropathol. Exp. Neurol., *59:* 333–337, 2000.
21. Zurawel, R. H., Chiappa, S. A., Allen, C., and Raffel, C. Sporadic medulloblastomas contain oncogenic β-catenin mutations. Cancer Res., *58:* 896–899, 1998.
22. Jia, J., Amanai, K., Wang, G., Tang, J., Wang, B., and Jiang, J. Shaggy/GSK3 antagonizes Hedgehog signalling by regulating *Cubitus interruptus*. Nature (Lond.), *416:* 548–552, 2002.
23. Hoeijmakers, J. H. Genome maintenance mechanisms for preventing cancer. Nature (Lond.), *411:* 366–374, 2001.
24. Jiricny, J., and Marra, G. DNA repair defects in colon cancer. Curr. Opin. Genet. Dev., *13:* 61–69, 2003.
25. Lee, Y., and McKinnon, P. J. DNA ligase IV suppresses medulloblastoma formation. Cancer Res., *62:* 6395–6399, 2002.
26. Tong, W. M., Ohgaki, H., Huang, H., Granier, C., Kleihues, P., and Wang, Z. Q. Null mutation of DNA strand break-binding molecule poly(ADP-ribose) polymerase causes medulloblastomas in *p53(−/−)* mice. Am. J. Pathol., *162:* 343–352, 2003.
27. Pazzaglia, S., Mancuso, M., Atkinson, M. J., Tanori, M., Rebessi, S., Majo, V. D., Covelli, V., Hahn, H., and Saran, A. High incidence of medulloblastoma following X-ray-irradiation of newborn *Ptc1* heterozygous mice. Oncogene, *21:* 7580–7584, 2002.
28. Hahn, H., Wojnowski, L., Zimmer, A. M., Hall, J., Miller, G., and Zimmer, A. Rhabdomyosarcomas and radiation hypersensitivity in a mouse model of Gorlin syndrome. Nat. Med., *4:* 619–622, 1998.
29. Aszterbaum, M., Epstein, J., Oro, A., Douglas, V., LeBoit, P. E., Scott, M. P., and Epstein, E. H., Jr. Ultraviolet and ionizing radiation enhance the growth of BCCs and trichoblastomas in *patched* heterozygous knockout mice. Nat. Med., *5:* 1285–1291, 1999.
30. Wetmore, C., Eberhart, D. E., and Curran, T. Loss of *p53* but not *ARF* accelerates medulloblastoma in mice heterozygous for *patched*. Cancer Res., *61:* 513–516, 2001.
31. Marino, S., Vooijs, M., van Der Gulden, H., Jonkers, J., and Berns, A. Induction of medulloblastomas in *p53*-null mutant mice by somatic inactivation of *Rb* in the external granular layer cells of the cerebellum. Genes Dev., *14:* 994–1004, 2000.
32. Cunningham, J. J., Levine, E. M., Zindy, F., Goloubeva, O., Roussel, M. F., and Smeyne, R. J. The cyclin-dependent kinase inhibitors *p19(Ink4d)* and *p27(Kip1)* are coexpressed in select retinal cells and act cooperatively to control cell cycle exit. Mol. Cell. Neurosci., *19:* 359–374, 2002.
33. Zindy, F., den Besten, W., Chen, B., Rehg, J. E., Latres, E., Barbacid, M., Pollard, J. W., Sherr, C. J., Cohen, P. E., and Roussel, M. F. Control of spermatogenesis in mice by the cyclin D-dependent kinase inhibitors *p18(Ink4c)* and *p19(Ink4d)*. Mol. Cell. Biol., *21:* 3244–3255, 2001.
34. Zindy, F., Cunningham, J. J., Sherr, C. J., Jogal, S., Smeyne, R. J., and Roussel, M. F. Postnatal neuronal proliferation in mice lacking *Ink4d* and *Kip1* inhibitors of cyclin-dependent kinases. Proc. Natl. Acad. Sci. USA, *96:* 13462–13467, 1999.

[7] R. Hernan, Y. Lee, P. J. McKinnon, R. J. Gilbertson, unpublished observation.

35. Gilbertson, R. J., Perry, R. H., Kelly, P. J., Pearson, A. D., and Lunec, J. Prognostic significance of HER2 and HER4 coexpression in childhood medulloblastoma. Cancer Res., *57:* 3272–3280, 1997.
36. Donehower, L. A., Harvey, M., Slagle, B. L., McArthur, M. J., Montgomery, C. A., Jr., Butel, J. S., and Bradley, A. Mice deficient for *p53* are developmentally normal but susceptible to spontaneous tumours. Nature (Lond.), *356:* 215–221, 1992.
37. Harvey, M., McArthur, M. J., Montgomery, C. A., Jr., Butel, J. S., Bradley, A., and Donehower, L. A. Spontaneous and carcinogen-induced tumorigenesis in *p53*-deficient mice. Nat. Genet., *5:* 225–229, 1993.
38. Jacks, T., Remington, L., Williams, B. O., Schmitt, E. M., Halachmi, S., Bronson, R. T., and Weinberg, R. A. Tumor spectrum analysis in *p53*-mutant mice. Curr. Biol., *4:* 1–7, 1994.
39. Goldowitz, D., and Hamre, K. The cells and molecules that make a cerebellum. Trends Neurosci., *21:* 375–382, 1998.
40. Downes, M., and Koopman, P. SOX18 and the transcriptional regulation of blood vessel development. Trends Cardiovasc. Med., *11:* 318–324, 2001.
41. Kato, K. Novel GABAA receptor α subunit is expressed only in cerebellar granule cells. J. Mol. Biol., *214:* 619–624, 1990.
42. Prescott, J. E., Osthus, R. C., Lee, L. A., Lewis, B. C., Shim, H., Barrett, J. F., Guo, Q., Hawkins, A. L., Griffin, C. A., and Dang, C. V. A novel c-Myc-responsive gene, *JPO1*, participates in neoplastic transformation. J. Biol. Chem., *276:* 48276–48284, 2001.
43. Frank, K. M., Sharpless, N. E., Gao, Y., Sekiguchi, J. M., Ferguson, D. O., Zhu, C., Manis, J. P., Horner, J., DePinho, R. A., and Alt, F. W. DNA ligase IV deficiency in mice leads to defective neurogenesis and embryonic lethality via the p53 pathway. Mol. Cell, *5:* 993–1002, 2000.
44. Barnes, E. A., Kong, M., Ollendorff, V., and Donoghue, D. J. *Patched1* interacts with cyclin B1 to regulate cell cycle progression. EMBO J., *20:* 2214–2223, 2001.
45. Rolig, R. L., and McKinnon, P. J. Linking DNA damage and neurodegeneration. Trends Neurosci., *23:* 417–424, 2000.
46. Gilbertson, R. J., Clifford, S. C., MacMeekin, W., Meekin, W., Wright, C., Perry, R. H., Kelly, P., Pearson, A. D., and Lunec, J. Expression of the ErbB-neuregulin signaling network during human cerebellar development: implications for the biology of medulloblastoma. Cancer Res., *58:* 3932–3941, 1998.
47. Ferrando, A. A., Neuberg, D. S., Staunton, J., Loh, M. L., Huard, C., Raimondi, S. C., Behm, F. G., Pui, C. H., Downing, J. R., Gilliland, D. G., Lander, E. S., Golub, T. R., and Look, A. T. Gene expression signatures define novel oncogenic pathways in T cell acute lymphoblastic leukemia. Cancer Cell, *1:* 75–87, 2002.
48. Yeoh, E. J., Ross, M. E., Shurtleff, S. A., Williams, W. K., Patel, D., Mahfouz, R., Behm, F. G., Raimondi, S. C., Relling, M. V., Patel, A., *et al.* Classification, subtype discovery, and prediction of outcome in pediatric acute lymphoblastic leukemia by gene expression profiling. Cancer Cell, *1:* 133–143, 2002.
49. Smyth, I., Narang, M. A., Evans, T., Heimann, C., Nakamura, Y., Chenevix-Trench, G., Pietsch, T., Wicking, C., and Wainwright, B. J. Isolation and characterization of human *patched 2* (*PTCH2*), a putative tumour suppressor gene in basal cell carcinoma and medulloblastoma on chromosome *1p32*. Hum. Mol. Genet., *8:* 291–297, 1999.
50. Armstrong, S. A., Staunton, J. E., Silverman, L. B., Pieters, R., den Boer, M. L., Minden, M. D., Sallan, S. E., Lander, E. S., Golub, T. R., and Korsmeyer, S. J. *MLL* translocations specify a distinct gene expression profile that distinguishes a unique leukemia. Nat. Genet., *30:* 41–47, 2002.
51. MacDonald, T. J., Brown, K. M., LaFleur, B., Peterson, K., Lawlor, C., Chen, Y., Packer, R. J., Cogen, P., and Stephan, D. A. Expression profiling of medulloblastoma: PDGFRA and the RAS/MAPK pathway as therapeutic targets for metastatic disease. Nat. Genet. *29:* 143–152, 2001.
52. Pomeroy, S. L., Tamayo, P., Gaasenbeek, M., Sturla, L. M., Angelo, M., McLaughlin, M. E., Kim, J. Y., Goumnerova, L. C., Black, P. M., Lau, C., *et al.* Prediction of central nervous system embryonal tumour outcome based on gene expression. Nature (Lond.), *415:* 436–442, 2002.
53. Zaphiropoulos, P. G., Unden, A. B., Rahnama, F., Hollingsworth, R. E., and Toftgard, R. *PTCH2*, a novel human patched gene, undergoing alternative splicing and up-regulated in basal cell carcinomas. Cancer Res., *59:* 787–792, 1999.
54. Carpenter, D., Stone, D. M., Brush, J., Ryan, A., Armanini, M., Frantz, G., Rosenthal, A., and de Sauvage, F. J. Characterization of two patched receptors for the vertebrate hedgehog protein family. Proc. Natl. Acad. Sci. USA, *95:* 13630–13634, 1998.
55. Ingram, W. J., Wicking, C. A., Grimmond, S. M., Forrest, A. R., and Wainwright, B. J. Novel genes regulated by Sonic Hedgehog in pluripotent mesenchymal cells. Oncogene, *21:* 8196–8205, 2002.
56. Uren, A., Reichsman, F., Anest, V., Taylor, W. G., Muraiso, K., Bottaro, D. P., Cumberledge, S., and Rubin, J. S. Secreted frizzled-related protein-1 binds directly to Wingless and is a biphasic modulator of Wnt signaling. J. Biol. Chem., *275:* 4374–4382, 2000.
57. Yoshino, K., Rubin, J. S., Higinbotham, K. G., Uren, A., Anest, V., Plisov, S. Y., and Perantoni, A. O. Secreted Frizzled-related proteins can regulate metanephric development. Mech. Dev., *102:* 45–55, 2001.
58. Duman-Scheel, M., Weng, L., Xin, S., and Du, W. Hedgehog regulates cell growth and proliferation by inducing cyclin D and cyclin E. Nature (Lond.), *417:* 299–304, 2002.
59. Kenney, A. M., Cole, M. D., and Rowitch, D. H. N-*myc* upregulation by sonic hedgehog signaling promotes proliferation in developing cerebellar granule neuron precursors. Development (Camb.), *130:* 15–28, 2003.
60. Ciemerych, M. A., Kenney, A. M., Sicinska, E., Kalaszczynska, I., Bronson, R. T., Rowitch, D. H., Gardner, H., and Sicinski, P. Development of mice expressing a single D-type cyclin. Genes Dev., *16:* 3277–3289, 2002.
61. Knoepfler, P. S., Cheng, P. F., and Eisenman, R. N. N-*myc* is essential during neurogenesis for the rapid expansion of progenitor cell populations and the inhibition of neuronal differentiation. Genes Dev., *16:* 2699–2712, 2002.
62. Zhao, Q., Kho, A., Kenney, A. M., Yuk Di, D. I., Kohane, I., and Rowitch, D. H. Identification of genes expressed with temporal-spatial restriction to developing cerebellar neuron precursors by a functional genomic approach. Proc. Natl. Acad. Sci. USA, *99:* 5704–5709, 2002.
63. Vousden, K. H., and Lu, X. Live or let die: the cell's response to p53. Nat. Rev. Cancer, *2:* 594–604, 2002.
64. Adesina, A. M., Nalbantoglu, J., and Cavenee, W. K. *p53* gene mutation and *mdm2* gene amplification are uncommon in medulloblastoma. Cancer Res., *54:* 5649–5651, 1994.
65. Burns, A. S., Jaros, E., Cole, M., Perry, R., Pearson, A. J., and Lunec, J. The molecular pathology of p53 in primitive neuroectodermal tumours of the central nervous system. Br. J. Cancer, *86:* 1117–1123, 2002.
66. Badiali, M., Iolascon, A., Loda, M., Scheithauer, B. W., Basso, G., Trentini, G. P., and Giangaspero, F. *p53* gene mutations in medulloblastoma. Immunohistochemistry, gel shift analysis, and sequencing. Diagn. Mol. Pathol., *2:* 23–28, 1993.
67. Wang, W., Kumar, P., Whalley, J., Schwarz, M., Malone, G., Haworth, A., and Kumar, S. The mutation status of *PAX3* and *p53* genes in medulloblastoma. Anticancer Res., *18:* 849–853, 1998.
68. Saylors, R. L., 3rd, Sidransky, D., Friedman, H. S., Bigner, S. H., Bigner, D. D., Vogelstein, B., and Brodeur, G. M. Infrequent *p53* gene mutations in medulloblastomas. Cancer Res., *51:* 4721–4723, 1991.
69. Raffel, C., Thomas, G. A., Tishler, D. M., Lassoff, S., and Allen, J. C. Absence of *p53* mutations in childhood central nervous system primitive neuroectodermal tumors. Neurosurgery, *33:* 301–305; discussion 305–306, 1993.
70. Woodburn, R. T., Azzarelli, B., Montebello, J. F., and Goss, I. E. Intense p53 staining is a valuable prognostic indicator for poor prognosis in medulloblastoma/central nervous system primitive neuroectodermal tumors. J. Neurooncol., *52:* 57–62, 2001.
71. Giordana, M. T., Duo, D., Gasverde, S., Trevisan, E., Boghi, A., Morra, I., Pradotto, L., Mauro, A., and Chio, A. *MDM2* overexpression is associated with short survival in adults with medulloblastoma. Neuro-oncology, *4:* 115–122, 2002.
72. Raffel, C., Jenkins, R. B., Frederick, L., Hebrink, D., Alderete, B., Fults, D. W., and James, C. D. Sporadic medulloblastomas contain *PTCH* mutations. Cancer Res., *57:* 842–845, 1997.
73. Wolter, M., Reifenberger, J., Sommer, C., Ruzicka, T., and Reifenberger, G. Mutations in the human homologue of the Drosophila segment polarity gene *patched* (*PTCH*) in sporadic basal cell carcinomas of the skin and primitive neuroectodermal tumors of the central nervous system. Cancer Res., *57:* 2581–2585, 1997.
74. Xie, J., Johnson, R. L., Zhang, X., Bare, J. W., Waldman, F. M., Cogen, P. H., Menon, A. G., Warren, R. S., Chen, L. C., Scott, M. P., and Epstein, E. H. Mutations of the *PATCHED* gene in several types of sporadic extracutaneous tumors. Cancer Res., *57:* 2369–2372, 1997.
75. Pietsch, T., Waha, A., Koch, A., Kraus, J., Albrecht, S., Tonn, J., Sorensen, N., Berthold, F., Henk, B., Schmandt, N., *et al.* Medulloblastomas of the desmoplastic variant carry mutations of the human homologue of Drosophila *patched*. Cancer Res., *57:* 2085–2088, 1997.
76. Dong, J., Gailani, M. R., Pomeroy, S. L., Reardon, D., and Bale, A. E. Identification of *PATCHED* mutations in medulloblastomas by direct sequencing. Hum. Mutat., *16:* 89–90, 2000.
77. Schmitt, C. A., Fridman, J. S., Yang, M., Baranov, E., Hoffman, R. M., and Lowe, S. W. Dissecting *p53* tumor suppressor functions *in vivo*. Cancer Cell, *1:* 289–298, 2002.